242
doi:10.1017/S1431927615013446 © Microscopy Society of America 2015

Accurate Interpolation of 3D Fields Close to the Optical Axis

Michal Horák[1] and Jakub Zlámal[1,2]

[1.] Institute of Physical Engineering, Brno University of Technology, Brno, Czech Republic.
[2.] CEITEC BUT, Brno, Czech Republic.

The rotational symmetry of a magnetic lens can be disrupted by holes drilled into the lens to allow e.g. an implementation of detectors in real electron optical systems. In this case, the field acting on electrons must be solved as fully 3D problem and software like COMSOL Multiphysics, Field Precision is necessary because the Sturrock's perturbation theory [1-3] cannot be applied to calculate the field of this lens geometry in two dimensions. The 3D field solution needs to be interpolated very precisely close to the optical axis but the precision of interpolation polynomials often suffer from the numerical errors of calculated field. Decomposition of the 3D field to multipole fields and subsequent determination of axial multipole field functions seems to be a powerful method for smooth and accurate interpolation of 3D fields. This is important for the evaluation of aberration integrals and for particle tracing. The presented method is demonstrated on saturated 200 kV magnetic objective lens of Tsuno [4], which is the standard example in EOD [5], with a hole drilled into the polepiece.

Radial expansion of axial field of rotationally symmetric and multipole magnetic fields can be easily derived from the Laplace equation for scalar magnetic potential. Power series for the scalar magnetic potential of N terms for every m-th multipole field component in basic configuration is

$$\Psi_m(r,\varphi,z) = \frac{1}{\mu_0}\sum_{i=0}^{N-1}(-1)^{i+1}\frac{1}{4^i}\frac{m!}{i!\,(m+i)!}\cdot D_m^{(2i)}(z)\cdot r^{2i+m}\cdot\cos(m\varphi), \tag{1}$$

with D_m as the m-th axial multipole field function. Consequently magnetic flux density is

$$\begin{aligned} B_r(r,\varphi,z) &= \sum_m C_{r,m}(r,z)\cdot\cos(m\varphi),\ C_{r,m}(r,z) \propto \sum_{i=0}^{N-1} D_m^{(2i)}(z)\cdot r^{2i+m-1},\\ B_\varphi(r,\varphi,z) &= \sum_m S_{\varphi,m}(r,z)\cdot\sin(m\varphi),\ S_{\varphi,m}(r,z) \propto \sum_{i=0}^{N-1} D_m^{(2i)}(z)\cdot r^{2i+m},\\ B_z(r,\varphi,z) &= \sum_m C_{z,m}(r,z)\cdot\cos(m\varphi),\ C_{z,m}(r,z) \propto \sum_{i=0}^{N-1} D_m^{(2i+1)}(z)\cdot r^{2i+m}. \end{aligned} \tag{2}$$

The process of determination of axial field functions from 3D field solution consists of three main steps repeated for all z coordinates along the axis. Components of the magnetic field (in cylindrical coordinates) are evaluated using built in interpolation methods of 3D software on several circles with increasing radius r but the same z position of their centers on the optical axis.

The magnetic field components on each circle are expanded into Fourier series with respect to Eq. (2), which means cosine series for B_r and B_z and sine series for B_φ. The calculation of Fourier coefficients $C_{r,m}$, $S_{\varphi,m}$ and $C_{z,m}$ as integrals over angular coordinate φ for each circle radius r also partially eliminates the fluctuation of the field due to numerical errors of the 3D field calculation.

https://doi.org/10.1017/S1431927615013446 Published online by Cambridge University Press

The axial multipole and rotationally symmetric (for $m = 0$) field functions $D_m(z)$ and their derivatives at the given z coordinate are obtained by the least squares fit of radial dependence of the Fourier coefficients $C_{r,m}(r,z)$, $S_{\varphi,m}(r,z)$ and $C_{z,m}(r,z)$ with respect to the power series (2). This least square fit eliminates the fluctuations of the 3D field interpolation in radial direction (e.g. Figure 2). Standard deviations $SD(D_m)$ of fitted axial field functions $D_m(z)$ are used as an index of quality of the least squares fit. Power series (2) can then be used to interpolate field near the optical axis for accurate particle tracing.

Numerical example

A magnetic objective lens (also discussed in [2]) with a hole drilled into the polepiece perpendicular to the optical axis will serve as the first example. The position of the hole is $z = -10$ mm and the diameter is 5 mm (Figure 1). As the second example we will use the same lens, but with the four identical holes drilled perpendicular to the optical axis with mutual span of 90 degrees. Calculated fields obtained in both examples are compared with the field of the lens without holes, i.e. perfectly rotationally symmetric lens. The magnetic lens is in all cases saturated and the excitation of the lens is 10500 ampere-turns. The sampling step for the axial field functions calculations is 0.01 mm in r direction and the range 0.01 mm to 0.5 mm. In z direction the step is 0.01 mm (range -20 to 10 mm) and 1 deg in φ coordinate. The first three terms of (2) are used for the least squares fit.

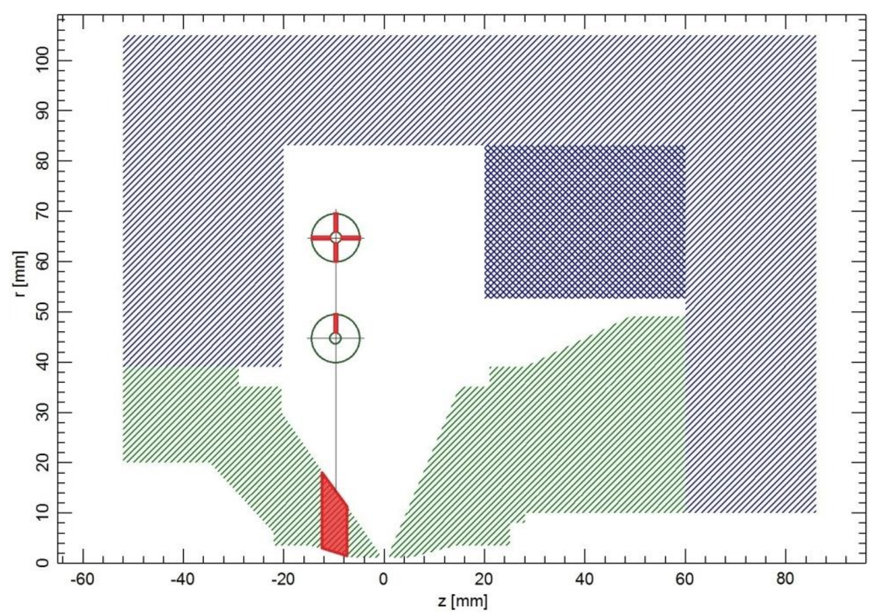

Figure 1. Saturated magnetic lens with one, respectively four holes drilled perpendicular to the optical axis. A schematic view on the polepiece cross section with indicated holes is also shown.

The smallest FEM mesh element size used for 2D calculation (performed in EOD) of the lens without hole is 0.05 mm in gap. In 3D calculation (performed in COMSOL Multiphysics) it was reduced to about 0.15 mm in the region close to the axis to achieve sufficient accuracy of the field, reasonable memory consumption and computation time. The most demanding part of the 3D calculation is the gap region where the field of the lens is almost 3 T whereas the multipole fields are weak, but important for the determination of the influence of the holes on optical properties. Using the smallest possible relative accuracy of field computation $5 \cdot 10^{-8}$, for which the solution still converges, the quadrupole and hexapole components of the flux density fields are noisy here due to numerical errors. The relative error

https://doi.org/10.1017/S1431927615013446 Published online by Cambridge University Press

of fitted axial field functions measured by standard deviation is below 1 % except the region of the lens gap, where the standard deviation of hexapole axial field component is 5 %.

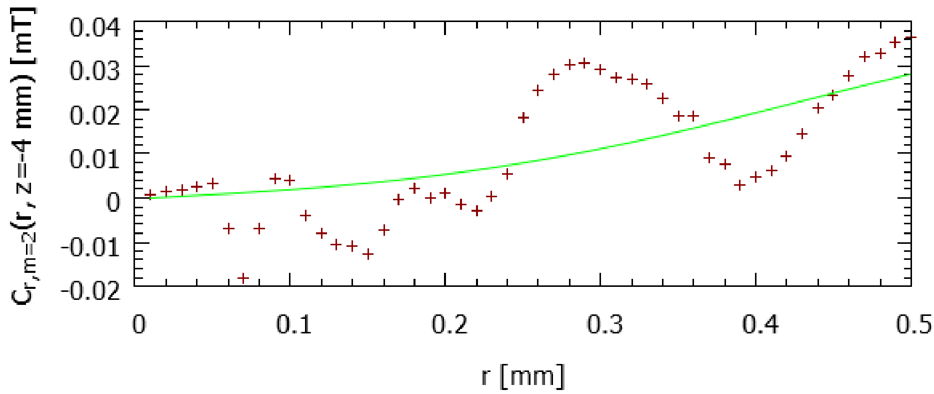

Figure 2. Magnetic lens with one hole – the least squares fit of the radial dependency of the Fourier coefficient $C_{r,2}$ for the radial quadrupole component of the magnetic flux density at $z = -4$ mm. As the quadrupole field is weak here the degree of noise in the 3D solution of the field is comparable with the field component itself.

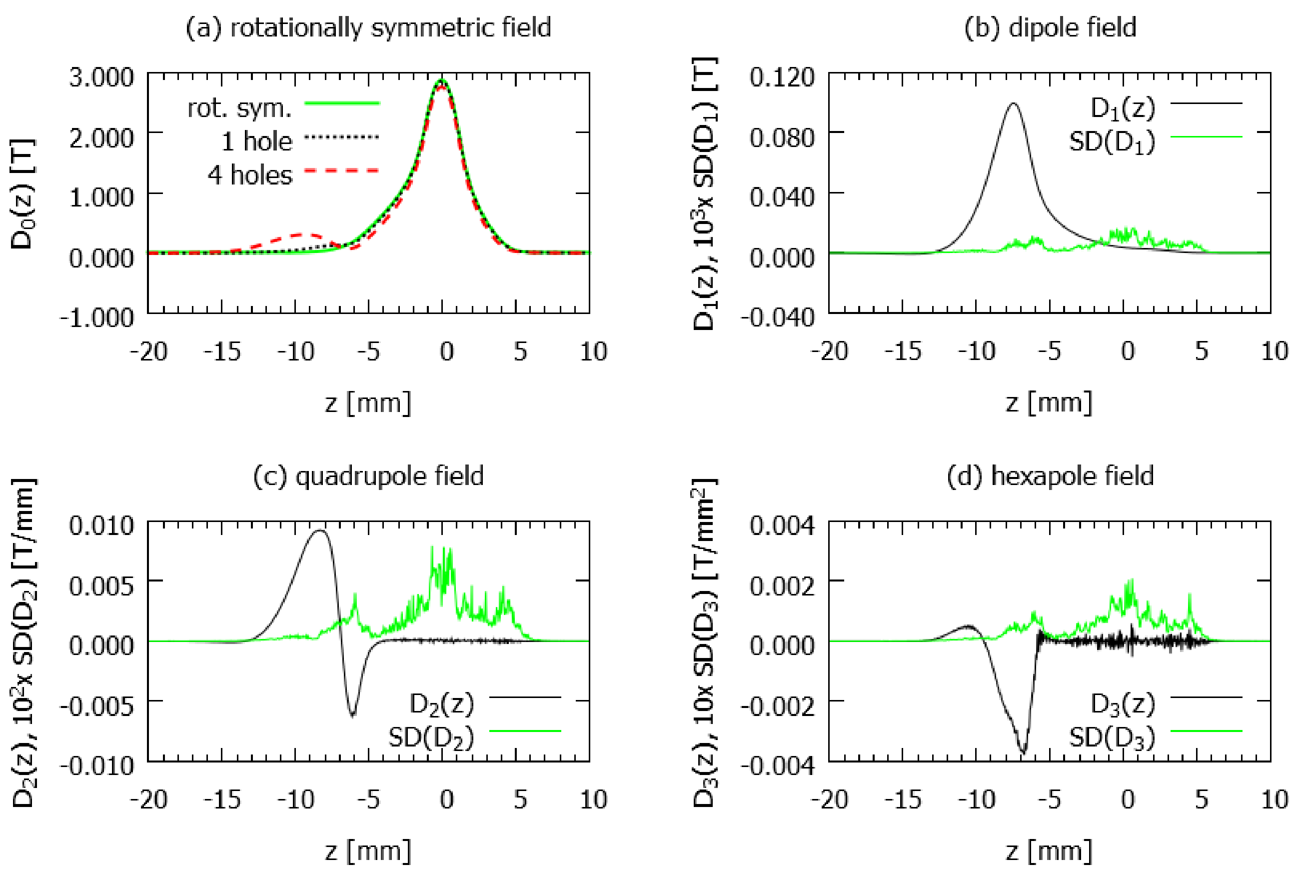

Figure 3. Axial field functions: (a) rotationally symmetric field components of all three cases. (b) dipole field component and its standard deviation 1000 times magnified, (c) quadrupole field component and its standard deviation 100 times magnified and (d) hexapole field component and its standard deviation 10 times magnified of the lens with one hole.

https://doi.org/10.1017/S1431927615013446 Published online by Cambridge University Press

One hole drilled into the polepiece of the lens causes a change of rotationally symmetric axial field not only in the vicinity of the hole (Figure 3a), but also results in additional multipole fields – dipole field (Figure 3b), weak quadrupole field (Figure 3c) and hexapole field (Figure 3d). Higher order multipole fields are either not present or below the noise level. These multipole fields are suppressed when the lens with four holes is used but missing material causes a great change of the rotationally symmetric axial field function compared to field of the lens without hole as can be seen in Figure 3a.

Axial multipole field functions are noisy, especially in the lens gap region, because no smoothing was used in the z direction. The regions with high degree of noise indicate the necessity of the use of more accurate 3D field calculation, i.e. the use of denser mesh. Unfortunately, the memory requirements for such calculation are too high. On the other hand, the smoothing of these axial multipole field functions can be performed e.g. using a de-noising process of a one-dimensional signal by wavelets which is useful for further calculations although it can change the shape of higher derivatives of axial field [6].

The basic optical properties of the studied lenses were evaluated for object at $z = -130$ mm and image in the center of the gap. The spherical aberration, beam deflection and axial coma were calculated using aberration integrals. The two-fold axial astigmatism was calculated by tracing and fitting aberration polynomial [2]. The spherical aberration is 0.59 mm for the rotationally symmetric lens, 0.58 mm for the lens with one hole and 0.60 mm for the lens with four holes. The multipole field components are present only in the lens with one hole. The beam deflection caused by the dipole field is 0.42 mm. The size of the axial coma is 0.50 mm. Finally the two-fold axial astigmatism, caused by the quadrupole field, is 0.38 μm.

Conclusion

The axial multipole components of magnetic field of 3D field of saturated magnetic lens can be determined using least squares method. Estimation of standard deviation of the axial field can be used as a natural test of the 3D field numerical error and also as an indicator of the volume where the mesh posses insufficient density. As a numerical example of method, axial multipole fields of the lens with the hole drilled into the polepiece were determined from the 3D solution of the field. These additional field components can be suppressed using the four-fold symmetry of the holes. Although the rotationally symmetric component of the magnetic field is significantly affected, the spherical aberration is similar. For further use of axial field functions as interpolation polynomial near optical axis it will be useful to implement the de-noising process in z direction [7].

References:

[1] PA Sturrock, Philos. Tr. R. Soc. S-A **243** (1951), p. 387.
[2] O Shánĕl, J Zlámal and M Oral, Ultramicroscopy **137** (2014), p. 1.
[3] J Zlámal and B Lencová, Nucl. Instr. Meth. A **645** (2011), p. 278.
[4] M Kato and K Tsuno, IEEE T. Magn. **26** (1990), p. 1023.
[5] B Lencová and J Zlámal, Phys. Procedia **1** (2008), p. 315.
[6] T Radlička and B Lencová, Ultramicroscopy **110** (2010), p. 1198.

[7] This research was financially supported by FEI Company and by European Regional Development Fund (CEITEC-CZ.1.05/1.1.00/02.0068).